Fabrication of Micro Porous Metal Components by Metal Injection Molding Based Powder Space Holder Method

Kazuaki Nishiyabu[1],# Satoru Matsuzaki[2] and Shigeo Tanaka[2]

[1] *Osaka Prefectural College of Technology,*
26-12 Saiwai, Neyagawa, Osaka 572-8572, Japan
[2] *Taisei-Kogyo Co., Ltd.,*
26-1 Ikeda-kita, Neyagawa, Osaka 572-0073, Japan

(Received April 2, 2006; final form April 15, 2006)

ABSTRACT

A novel production method for the metal components with micro-sized porous structures has been developed by applying the powder space holder (PSH) method to the metal powder injection molding (MIM) process. This production method is compatible with widespread applications with high functionality such as heat sinks, electrodes and medical implants and so on. These applications can benefit from the advantages provided by micro-porous metal components with complicated shapes using most kinds of metal powder. The aim of this study is to clarify the effects of material combinations and production conditions on the pore formation and some physical properties of sintered porous metals. The green compacts were molded via uniaxial hot pressing for an experiment using various porous compounds which were prepared by changing the combinations in size of stainless steel 316L powder and polymethylmethacrylate (PMMA) space holding particle. Afterwards they were sintered at various temperatures after thermal debinding. It was confirmed that the size of metal powder and space holding particle together with the sintering temperature were main factors affecting the pore size, porosity, surface area and shrinkage of sintered porous metals. It was concluded that the PSH-MIM method proposed was useful for producing metal components with micro-sized and high functionally porous structures.

Keywords: Porous metal, Metal injection molding, Space holder method, Porosity, Pore size

1. INTRODUCTION

Porous metal materials such as metal foams, cellular metals and metal sponges have been widely studied and used /1-3/. They are a new class of materials with low density, large specific surface and a range of novel properties in the physical, mechanical, thermal, electrical and acoustical field. Closed cell foams could potentially be used in applications that need light weight structural elements with better sound and impact energy absorption. Open cell foams also provide possibilities for high-functional applications such as heat exchangers and heat sinks for thermal management, but also for medical implants, filters and electrodes for biological

#Correspondence to Prof. K. Nishiyabu
E-mail: kazu@ipc.osaka-pct.ac.jp

and chemical reactions. In general, the cell size will be reduced as the size of products decrease from meters to millimeters as shown in Fig.1. So far, few studies have been dealing with net-shape production of micro-porous metal components which are strongly desired to produce applications with higher functionalities at a lower cost.

Fig.2 shows the ranges of porosity and cell type against cell size for typical production methods for metal foams /3/. These products can be manufactured with existing commercial production methods such as sintering of hollow spheres or metal textiles, melt gas injection in liquid metal, gas forming particle decomposition in semi-solid metal, vapor or electron-deposition method, entrapped gas expansion method and sintering of metal powders. Each method can be used with a small subset of methods to create porous materials with a limited range of porosity and cell size. In practice, it is very difficult to produce porous metal components with cell sizes controlled up to a few tens of micrometers and arbitrarily select both open and closed cell structures with a specified porosity. At the moment, few methods can produce net-shaped metal components with high production efficiency. Furthermore, porous materials with high densities are very promising to get a high specific modulus and high functionality. As discussed before, in practice it is not so easy to control the cell size or the cells distribution. It will be even more complicated to produce porous material with graded properties and complex shapes.

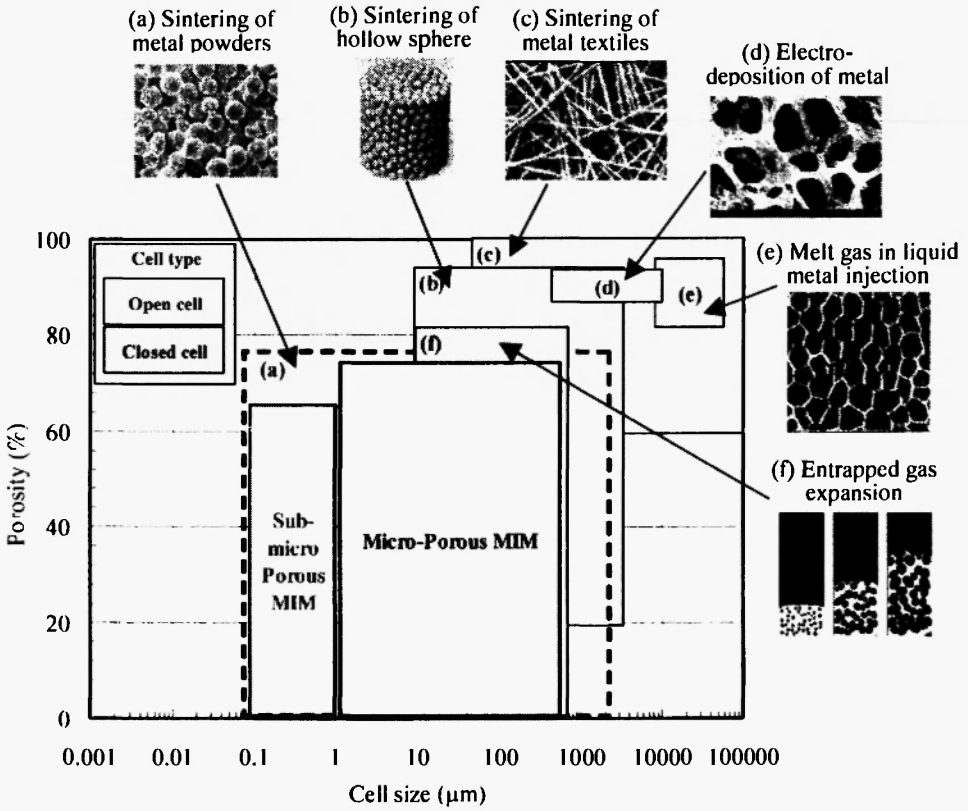

Fig.1: Scale in product and cell size of porous metals.

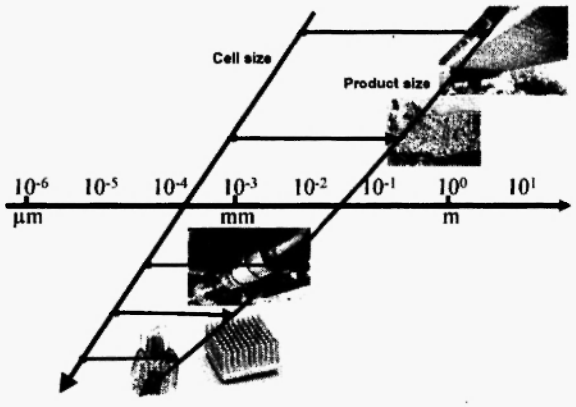

Fig.2: Porosity against cell size for typical production methods of porous metals.

Metal injection molding (MIM) is a manufacturing method that combines traditional powder metallurgy (P/M) with plastic injection molding as shown in Fig.3. Over the past decade it has established itself as a competitive manufacturing process for small precision components that would be costly to produce by alternative methods. It can be used to produce comparatively small parts with complex shapes from almost all types of materials like metals, ceramics, inter-metallic compounds, and composites /4, 5/. Recently MIM has been studied not only for hard metals, but also for materials such as titanium, copper and aluminum /6/. Unlike in the case of powder metallurgy, MIM requires mixing metal powders with a polymeric binder. Afterwards the organic constituents are removed in a debinding step such as solvent extraction or pyrolysis. These processes are unique for MIM. Therefore we should make better use of these processes, which does not have a little segregation between metal powder and binder. This is one of the reasons why we have developed a production method for micro-porous metal components based on the MIM process. We have tried to produce metal components with a micro-sized porous structure by applying the powder space holder (PSH) method to the MIM process /7-9/.

In this study, micro-porous metal components were produced by the PSH method combined with the MIM process. The effects of material combination and sintering conditions on the pore formation and the physical properties of sintered porous metals were investigated.

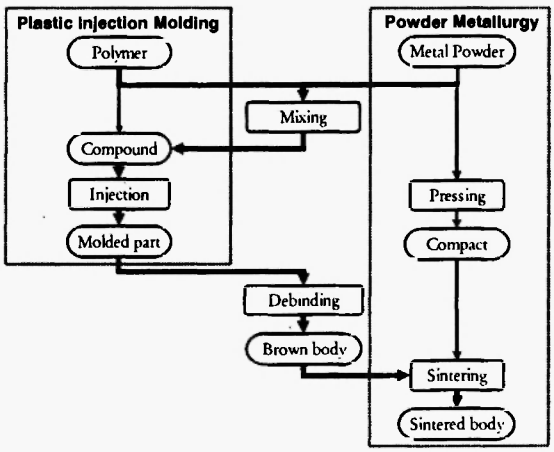

Fig.3: Flow of MIM process.

2. CONCEPT

2.1 MIM-based powder-space holder method

The concept of the production method for micro-porous metals we developed was based on the MIM process illustrated in Fig.4. In a conventional MIM process, the feedstock is composed of metal powder and binders. A high densification after debinding and the type of sintering process are very important for high quality MIM products. To produce highly porous structured metals, on the other hand, many spaces are

required to hold after sintering. We therefore have applied the PSH method to the MIM process. In addition to metal powder and thermoplastic binders, extra coarse spherical materials made of plastics were used as lost material to obtain a fine porous structure in MIM components. The combination of space holding particles and metal powder together with the sintering conditions determine the porous structure. This production method can be applied for application in heat sinks, electrodes and medical implants and so on. The main advantage of the proposed method is net-shape production of micro-porous metal components with complicated three-dimensional shapes and high functionally graded structures. This production method can be applied to most kinds of metal powder such as stainless steels, aluminum, copper, titanium, nickel and their alloys.

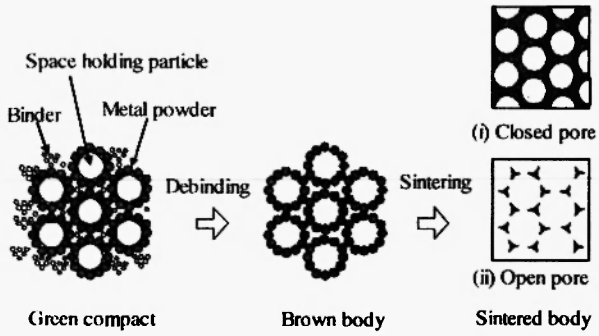

Fig.4: Powder space holder method for producing micro-porous metals.

2.2 Debinding mechanism

The key technology in the PSH method is to remove the space holding particles that were needed to make spherical spaces. The simplified debinding mechanism is shown for the case of a two components binder system. Fig.5(a) shows the typical debinding and sintering conditions for 9μm stainless steels powder. Debinding was done at 200°C during 2hr while sintering was carried out at around 1050°C during 2hr. Fig.5(b) shows the thermo-gravimetric curves for decomposition of the binder, wax, polymer and poly-methylmethacrylate (PMMA) particles can be used for this.

Fig.6 shows a schematic drawing of the debinding process at each temperature. Below 100°C no materials decompose yet, but at 250°C the wax starts to decompose, and it creates many paths for degassing near the PMMA particle. Then, at 300°C, the PMMA decomposes along with the wax. When the temperature is further increased to 350°C, large amounts of PMMA and Polymer decompose simultaneously. Finally, over 500°C, all binder constituents and PMMA particles have been decomposed. The previous description can be considered as the typical debinding mechanism for this material system.

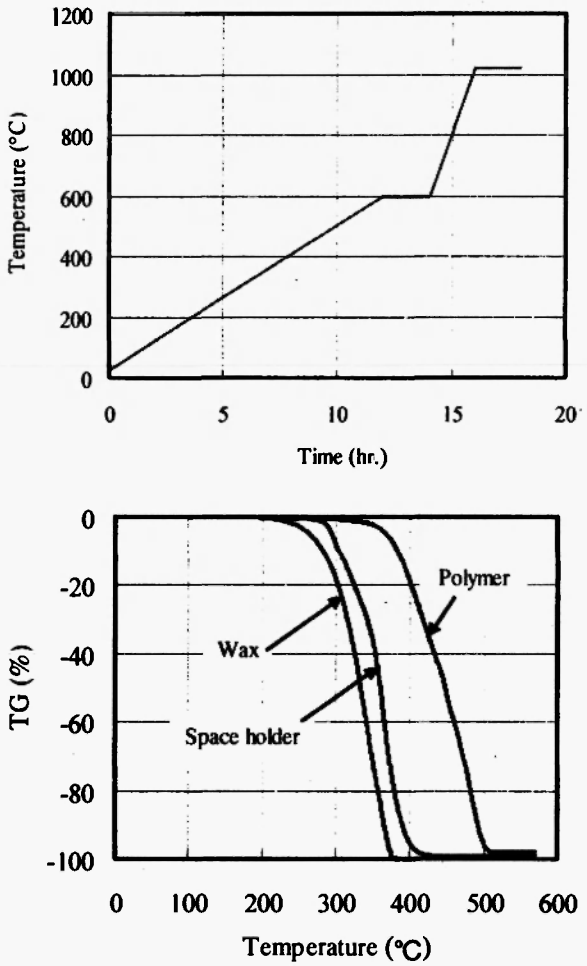

(a) Debinding-Sintering conditions. (b) TG curves in debinding.

Fig.5: Powder space holder method for producing micro-porous metals.

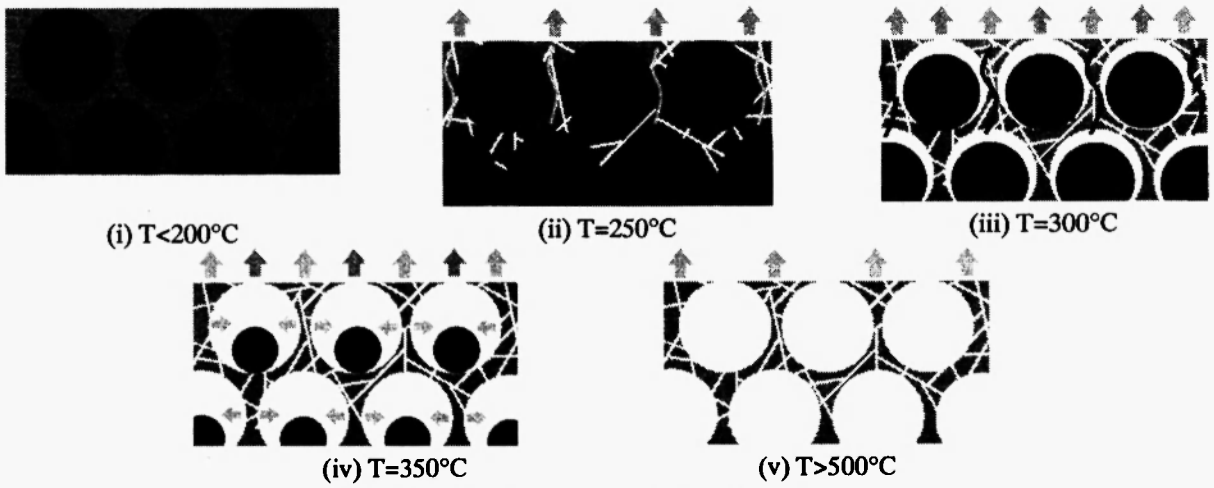

Fig.6: Schematic drawing of debinding process.

3. EXPERIMENTAL

3.1 Materials and porous compounds

The experimental materials used for porous compounds have been listed in Table 1. The metal powders are austenitic stainless steel 316L produced by the water-atomization method. The binder is from the polyacetal family. Spherical particles (10μm or 50μm in mean diameter) made from PMMA were used for holding the metal powder in position. These materials were co-mixed and pelletized with a high-pressure kneader and a plunger-type extruder. The resultant specimens are labeled Specimen 3-10 or Specimen 3-50. In the first case10μm PMMA particles together with 3μm of 316L powder were used. For the second specimen 50μm PMMA particles were mixed with 3μm of 316L powder. Specimen 9-50 is produced from 50μm of PMMA particles with 9μm of 316L powder. The fraction of PMMA particles varied from 0 to 80vol.% being the main experimental parameter.

3.2 Preparation conditions and evaluation

To keep the experiments simple, circular dishes of green compacts (40mm diameter, 2mm thick) were prepared from various porous compounds with the hot press molding process. The samples could also be produced by injection molding /6, 8/. The hot press molding was carried out under constant conditions where die temperature was 200°C and gage pressure was 10MPa, respectively. Debinding and sintering were sequentially carried out at 600°C for 2hr in N_2 and at 1050-1200°C for 2hr in an Ar gas atmosphere to avoid oxidizing.

The relative density (the inverse of porosity), and the shrinkage of the sintered specimens were measured with micrometer calipers and an analytical balance. The pore size, the pore distribution, the surface area and the flow resistance of a fluid through the sample were measured with a porometer (PMI, CPF-1100-AXLSP). The Surface structure of the sintered specimens was also observed by SEM (JEOL, JSM-6390LA).

Table 1
Experimental materials and fraction of constituents.

	Compositions	Mean diameter	Volume fraction	
			MIM feedstock	Porous compound
Metal powder	Stainless steel,316L	3μm	50vol.%	20-100vol.%
		9μm		
Binder	Wax, Polyacetal	-----	50vol.%	
Space holding particle	PMMA	10μm	-----	0-80vol.%
		50μm		

4. RESULTS AND DISCUSSIONS

4.1 Surface structures

The microstructures on the surface of sintered specimens produced by using various porous compounds are shown in Fig.7. The number of pores on the surface increases as the fraction of PMMA particles increases from 0 to 80vol.%. The pore size is significantly dependent on the diameter of PMMA particles. These characteristics are typical for pore formation behavior of the PSH method. To make micro-sized porous stainless steel with a much higher surface-to-volume ratio, it is better to take the compounds with combination of 3μm 316L powder and 10μm PMMA particles.

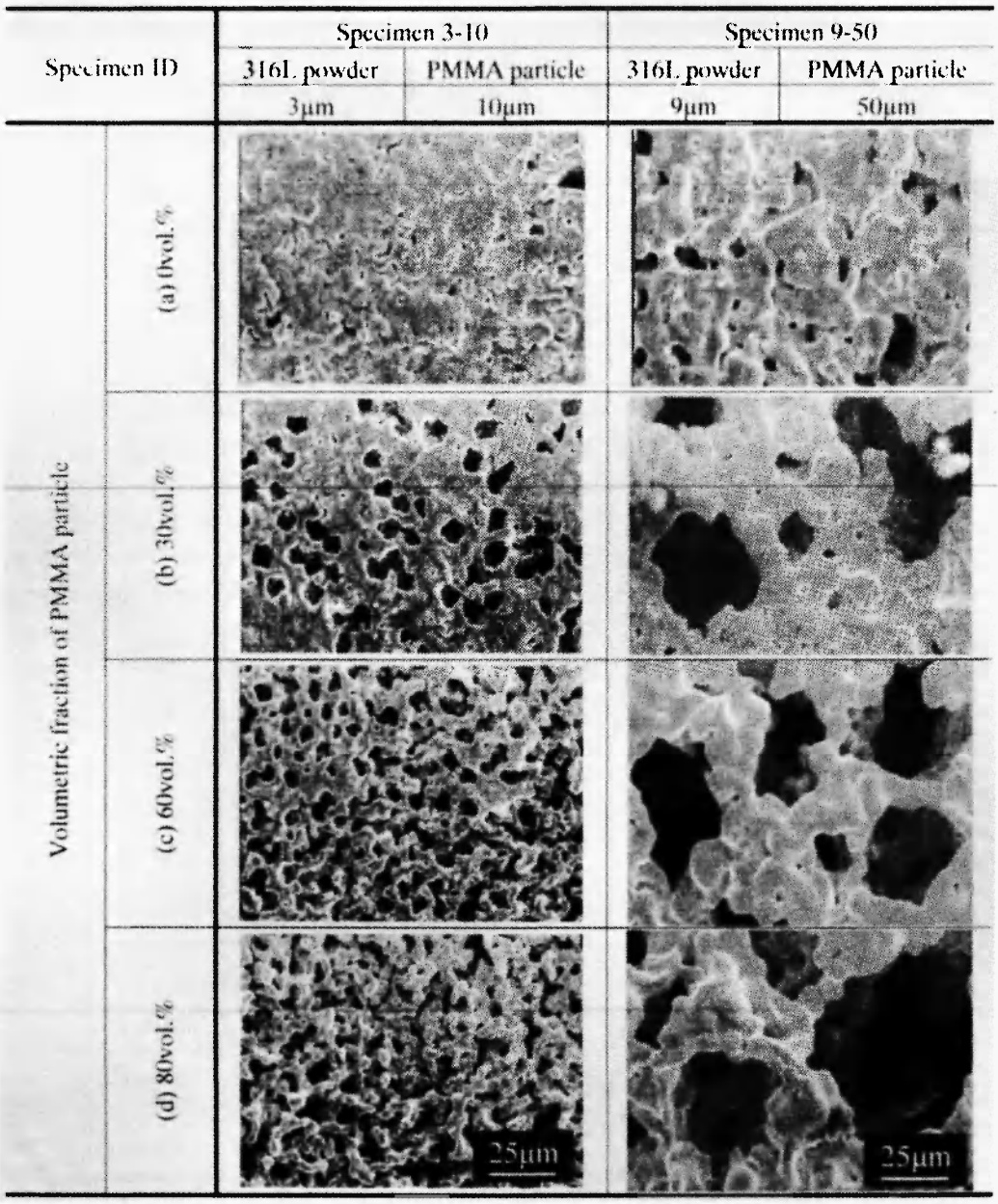

Fig.7: SEM images on surface of sintered specimens with various sizes of metal powder and PMMA particle.

4.2 Sintering shrinkage and porosity

Fig. 8 shows the shrinkage and the porosity of sintered porous specimens with various fractions of PMMA particles. The specimens 3-10 and 9-50 were sintered at 1050°C and 1200°C, respectively. For both specimens, the shrinkage is between 15-20% up to 50-60vol.% of PMMA particles. However, it increases rapidly when the fraction of PMMA particles becomes higher than 50-60vol%. It is considered that the transition point corresponds to the change from a closed cell structure to an open cell one. In other words, the shrinking percentage stays constant in a closed cell structure regardless of the content of PMMA particles. In an open cell structure, the shrinking percentage will increase when the fraction of PMMA particles rises. Then the definite transition points are shown at boundary between the closed cell structure and open cell structure. In the second graph the porosity of both specimens increases as the fraction of PMMA particles increases. Also here, two regions can be distinguished with a transition point between them. This result is similar to the first graph, where the shrinkage was plotted versus the fraction of PMMA particles

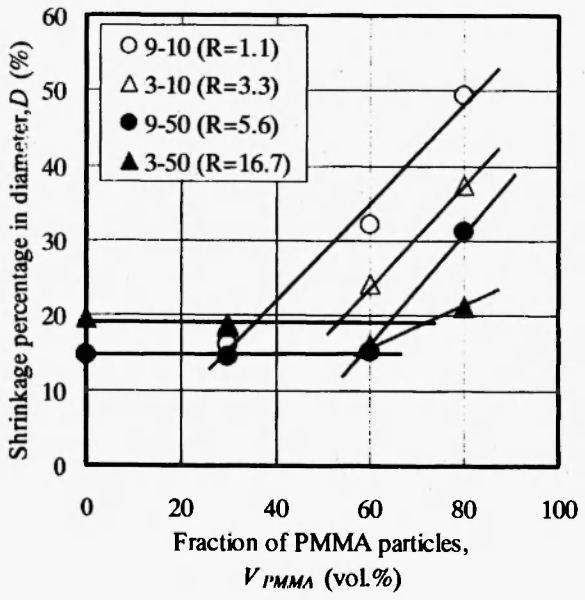

(a) Shrinkage diameter.

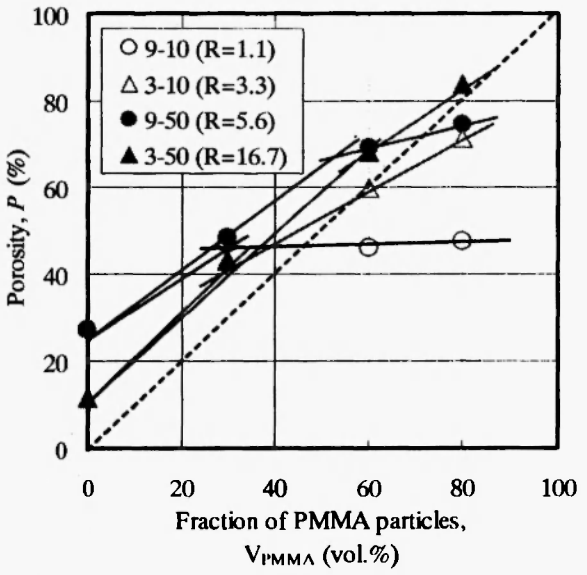

(b) Porosity.

Fig.8: Shrinkage and porosity as function of fraction of space holding particle.

The distribution of pore size for sintered specimens with various sizes of PMMA particles are shown in Fig.9. The pore size and the specific surface have been listed in Table 2. As the PMMA particle size decreases, the average diameter of the pore decreases accordingly, but the specific surface increases significantly. As a result, the average diameter of the pores was approximately equal to one quarter of the diameter of the PMMA particle.

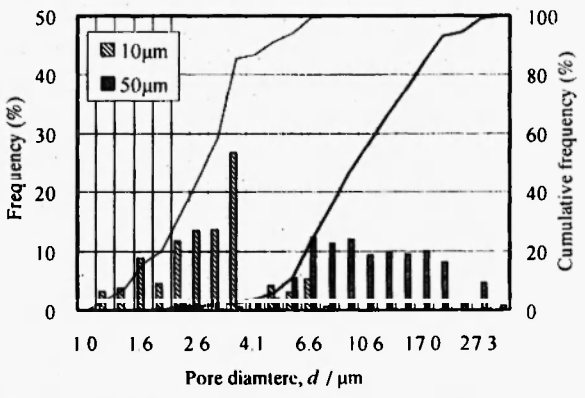

Fig.9: Distributions of pore size of sintered specimens with variant sizes of PMMA particle.

Table 2
Pore size and surface area of porous specimens with variant space holding particles.

	Specimen 9-50		Specimen 3-10	
	316L powder	PMMA particle	316L powder	PMMA particle
	9μm	50μm	3μm	10μm
Average diameter of pore	9.58μm		2.39μm	
Specific surface	$0.04m^2/g$		$0.15m^2/g$	

4.3 Effects of sintering temperature

Fig. 10 shows the shrinkage percentage in diameter and porosity for porous specimens with 60vol.% PMMA particles which were sintered at various temperatures. These results showed that the shrinkage increased and the porosity decreased accordingly in all specimens when the sintering temperature was increased. These phenomena agree with findings that the pore size tends to get smaller when the specimen undergoes an excess sintering. The shrinkage percentage in diameter is ideally 20% which is calculated by solid loading of MIM feedstock, i.e. 50vol.%. Therefore, when the sintering temperature is set at 1050°C for 3μm 316L-10μm PMMA (Specimen 3-10), 1200°C for 3μm 316L-50μm PMMA (Specimen 3-50), and 1300°C for 9μm316L-50μm PMMA (Specimen 9-50), the shrinkage percentage in diameter will be close to 20%, then the porosity could be achieved as close as the adding content of PMMA particle, i.e. 60vol.%. Then it can be concluded that porous structures with equally sized pores can be obtained under the above-cited sintering conditions for each combination of sizes of metal powder and space holding particles. Furthermore, it is revealed that sintering is more active in finer metal powder at higher sintering temperatures, and small pores exist additionally between metal particles by insufficient sintering in 50μm PMMA specimens (specimens 3-50 and 9-50), while cellular pore resulting from space holding particle affects remarkably by sintering temperature in 10μm PMMA specimen (specimen 3-10).

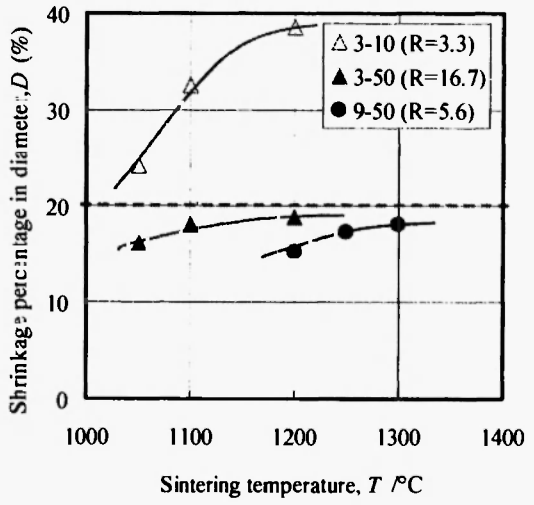

(a) Shrinkage in diameter.

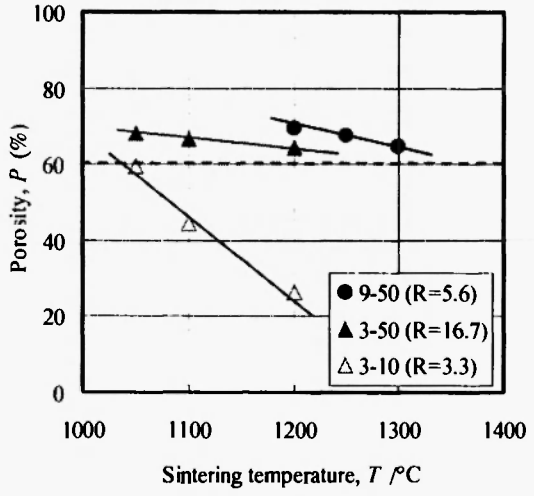

(b) Porosity.

Fig.10: Shrinkage and porosity as function of sintering temperature (60vol.% PMMA).

The effects of sintering temperature on the porous structural characteristics in the case of 3μm 316L-10μm PMMA specimens (Specimen 3-10) were investigated more in detail. The distributions of the pore size for specimens sintered at various temperatures are shown in Fig.11. At lower sintering temperatures such as 1020°C, the mean pore size is 1.65μm but it has a broad distribution. At higher sintering temperatures like 1070°C, the mean pore size was unchanged at 1.62μm, but the distribution becomes much sharper. This is considered as results of progress in sintering between

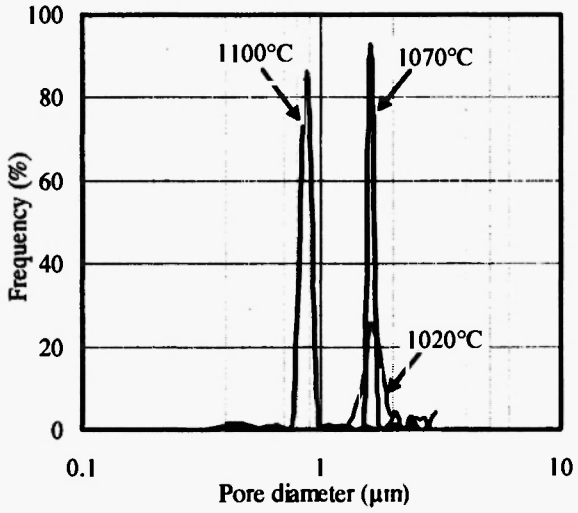

Fig.11: Distributions of pore size of specimens sintered at various temperatures (3μm 316L, 10μm PMMA (60vol.%)).

metal powders surrounding large pores held by space particle. When the sintering temperature is increased to 1100°C, the mean size was significantly reduced to 0.91μm but the sharp distribution remained. This is due to densification and can be seen on SEM images from the surface of specimens sintered at various temperatures as shown in Fig.12.

The surface area of specimens sintered at various temperatures was measured and shown in Fig.13. Specific surface decreases linearly with increasing sintering temperature. Also the resistance of a fluid to flow in specimens sintered at various temperatures was measured as shown in Fig.14. Specific water flow reduced significantly as the sintering temperature increased. These results are compatible with a decreasing of pore size in specimens sintered at higher temperature as discussed previously.

4.4 Geometrical analysis

The transition point between closed cell structures and open cell structures as function of the fraction of PMMA particles can be estimated by simple

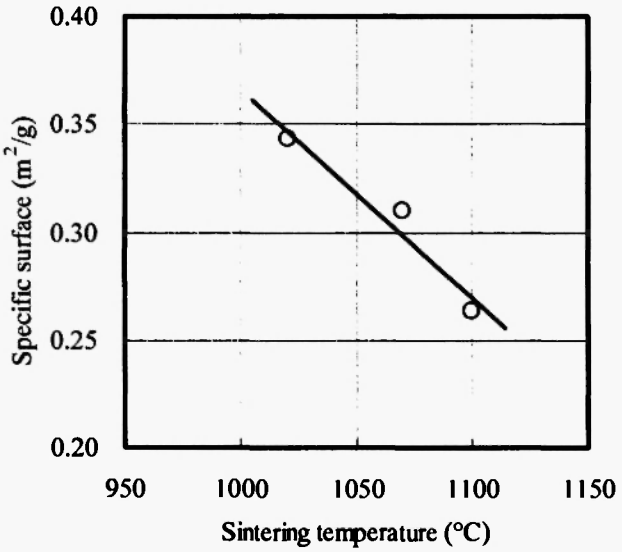

Fig.13: Specific surface as function of sintering temperature (3μm 316L, 10μm PMMA (60vol.%))

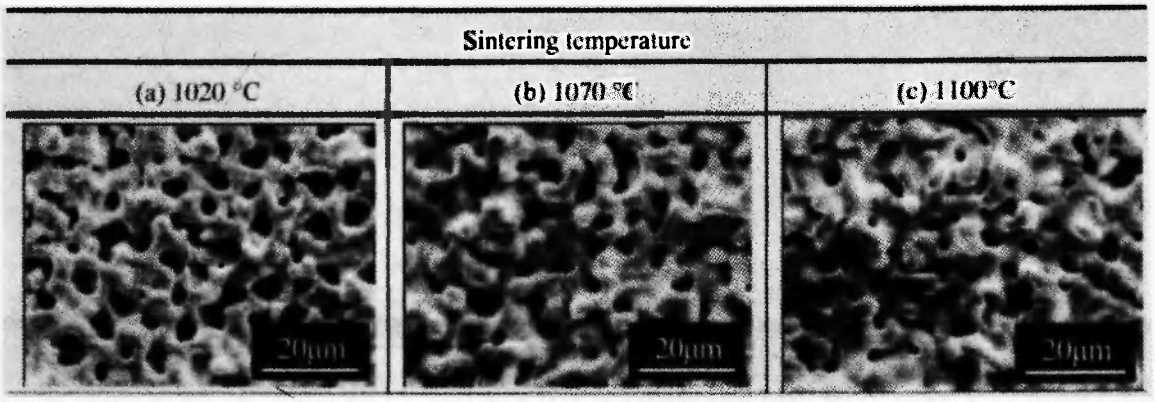

Fig.12: SEM images on surface of specimens sintered at various temperatures (3μm 316L, 10μm PMMA (60vol.%)).

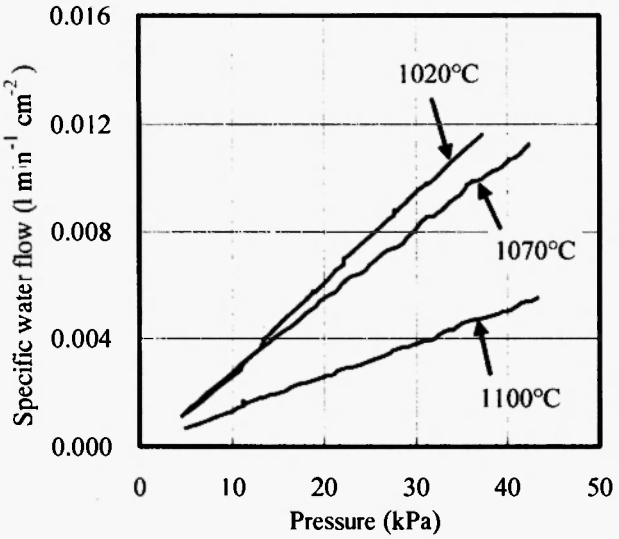

Fig.14: Specific water flow as function of sintering temperature (3μm 316L, 10μm PMMA (60vol.%))

geometrical analysis. When assuming that the metal powders are uniformly located around a PMMA particle, it can be modeled as a spherical PMMA particle coated by a single layer of metal powder as shown in Fig.15.

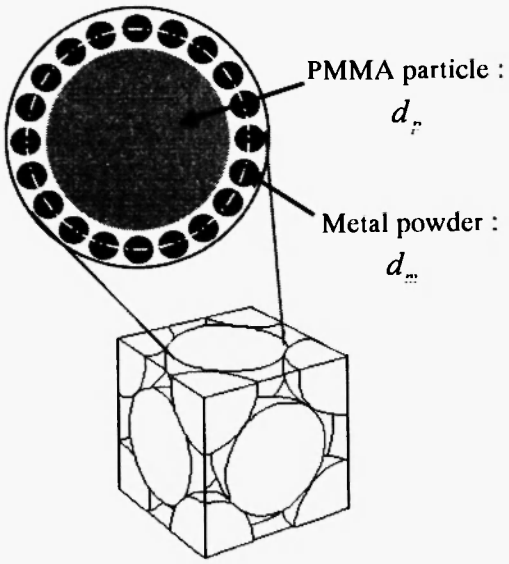

Fig.15: Geometrical model of face centered cubic structure in PMMA particles surrounded uniformly by metal powder.

When the spheres are closed-packed in a face centered cubic (fcc) structure, the volumetric fraction of PMMA particle reaches its maximum for the closed pore structure. The maximum fraction of PMMA particles, $(V_{PMMA})_{max}$, can be derived from Eqn. 1 as follows:

$$(V_{PMMA})_{max} = \frac{4 \times \frac{4}{3}\pi\left(\frac{d_p}{2}\right)^3}{\left\{\sqrt{2}(d_p + d_m)\right\}^3} \quad (1)$$

where, d_p is the mean diameter of a PMMA particle and d_m is the mean diameter of 316L powder.

The maximum fraction of PMMA particles for a closed cell structure was estimated by geometrical analysis and was then compared to the transition points as fraction of PMMA particles obtained from experimental results. The shrinkage percentage and the porosity for specimens with various size ratios of particle is shown in Fig.16 (a) and (b), respectively. The fractions of PMMA particles at these transition points were plotted for several ratios of particle size, R as shown in Fig.16. For comparison, the maximum fraction of PMMA particle estimated by Eqn.1 is drawn together with the curve in Fig.16. The curve indicates the boundary between closed cell and open cell structures. As can be seen, the experimental results agreed well with the curve estimated by geometrical analysis.

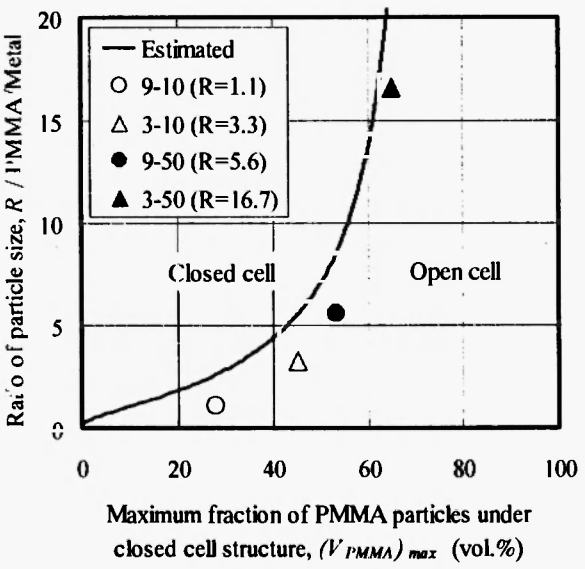

(a) Transition point in shrinkage in diameter.

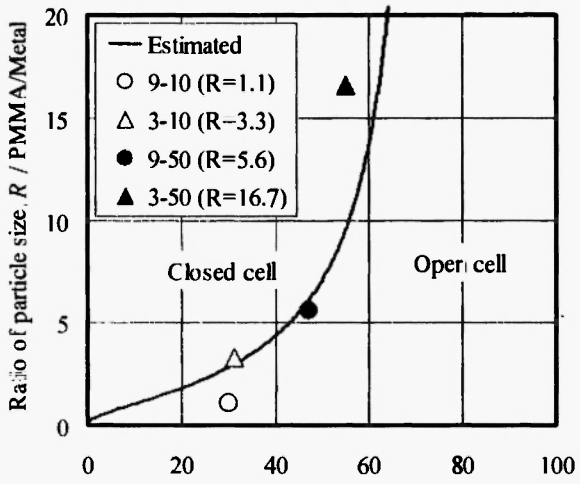

(b) Transition point in porosity.

Fig.16: Size ratio of PMMA particle/Metal powder versus maximum fraction of PMMA particle under closed cell structure.

5. CONCLUSIONS

The manufacturing method for micro-porous metal components using a powder space holder method together with a metal injection molding process was presented in this study. From experimental results and simple geometrical analysis, it was concluded that porous metals with micro-sized pores could be formed homogeneously when two parameters were optimized. First was the particle size of the spherical materials supporting the metal powder and secondly, the sintering temperature. The porosity could be easily controlled by the fraction of PMMA particles for space holding. The pore size is dependent on the particle size of PMMA. Surface area and resistance of a fluid to flow through sintered porous metals are significantly affected by the sintering temperature. Our method could be applied with injection or extrusion moldings for the net-shaped production of micro-porous metal components with complex three-dimensional shapes.

REFERENCES

1. L. J. Gibson and M. F. Ashby, *Cellular Solids - Structure & Properties*, Pergamon Press (1988).
2. M. F. Ashby, A. Evans, N. A. Fleck, L. J. Gibson, J. W. Hutchinson and H. N. G. Wadley, *Metal Foams, A Design Guide*, Elsevier Science (2000).
3. H. N. G. Wadley, *Cellular Metals Manufacturing, Advanced Engineering Materials*, **4**, 10 (2002).
4. R. M. German, *Powder Metallurgy Science*, 2nd edition, Metal Powder Industries Federation (1984).
5. R. M. German and A. Bose, *Injection Molding of Metals and Ceramics*, Metal Powder Industries Federation (1997).
6. K. Nishiyabu, S. Matsuzaki, M. Ishida, S. Tanaka and H. Nagai, Development of Porous Aluminum by Metal Injection Molding, *Proceedings of the 9th International Conference of Aluminum Alloy (ICAA-9)* (2004) p.376-382.
7. K. Nishiyabu, S. Matsuzaki, K. Okubo, M. Ishida and S. Tanaka, Porous Graded Materials by Stacked Metal Powder Hot-Press Molding, Materials, *Materials Science Forum*, Vols. 492-493 (2005) p.765-770.
8. K. Nishiyabu, S. Matsuzaki and S. Tanaka, Production of High Functionally Micro Porous Metal Components by Powder Space Holder Method, *Proceedings of International Symposium Cellular Metals for Structural and Functional Applications – CELLMET* 2005 (2005) p.41.
9. K. Nishiyabu, S. Matsuzaki and S. Tanaka, Production of Micro Porous Metal Components by Metal Injection Molding Based Powder Space Holder Method, *Proceedings of the 4th International Conference on Porous Metal and Metal Foaming Technology (MetFoam 2005)*, B55 (2005).